https://doi.org/10.17221/167/2020-VETMED

New perspectives in a microstructure study of the bovine and bubaline claw

Bruno Moraes Assis[1], Luisa Pucci Bueno Borges[2], Kleber Fernando Pereira[3], Caroline Rocha de Oliveira Lima[4], Luiz Antonio Franco da Silva[1], Pedro Paulo Maia Teixeira[2], Rogerio Elias Rabelo[3]*

[1]*Veterinary and Animal Science School, Goiás Federal University, Goiânia, GO, Brazil*
[2]*Veterinary Institut, Pará Federal University, PA, Brazil*
[3]*Veterinary Hospital, Goiás Federal University, Regional Jataí, Jataí, GO, Brazil*
[4]*Veterinary Science School, Goiás State University of Jataí Campus, Jataí, GO, Brazil*

**Corresponding author: bruno.moraes.assis@gmail.com*

Citation: Assis BM, Borges LPB, Pereira KF, de Oliveira Lima CR, da Silva LAF, Teixeira PPM, Rabelo RE (2022): New perspectives in a microstructure study of the bovine and bubaline claw. Vet Med-Czech 67, 395–407.

Abstract: The techniques of microtomography (Micro-CT), confocal laser scanner microscopy (CLSM), atomic force microscopy (AFM), nanoindentation – Vickers hardness (Nano-VH) and X-ray fluorescence (XRF) are undeniably important to the modern study of bovine podiatry. These techniques are also employed in engineering, physics and in the assessment of biomaterials used in reconstructive or experimental surgeries in bovine and bubaline claws. Although studies involving these analyses are still inconspicuous in veterinary medicine, these technologies represent a new paradigm in this area, enabling the development of new lines of research. The objective of this review is to gather information about the microstructural aspects of bovine and bubaline claws, concerning the intratubular and extratubular keratin, which is responsible for the physical and mechanical structure of the claw capsule. This study elucidates different methods used to evaluate the hooves of healthy and sick animals through a micrometric analysis and nano-scale analyses. We would like to emphasise that the described techniques can be applied to study other species.

Keywords: atomic force microscopy; confocal laser scanner microscopy; microtomography; nanoindentation; X-ray fluorescence

Introduction

For more than three decades, researchers around the world have been trying to understand the events related to bovine podiatry. It is a complex and challenging issue, and studies are always focused on applied aspects, including the classification of foot diseases, aetiopathogenesis, biosafety measures, treatment and disease control. Thus, a lack of knowledge and a scarcity of data related to basic areas have become a problem for researchers and the morpho-physiological features related to the vulnerability of the bovine claw became misunderstood and did not have enough scientific support to completely elucidate the origins and triggers of foot affections. In order to reverse this situation, studies have been redirected, revisiting the basic area and conducting scientific investigations involving bovine claw biometrics, radiography, tomography, thermography and venography (Silva 2012; Loureiro 2013; Freitas 2015). In addition, more complete and clear studies have been started, focusing on the claw microstructure, especially on the molecular and atomic levels (Assis et al. 2017a; Assis et al. 2017b).

https://doi.org/10.17221/167/2020-VETMED

Within new perspectives in studying bovine foot diseases, innovative techniques have been introduced that are barely used in veterinary medicine or not at all, including in physics, materials engineering and chemistry, making this subject a multidisciplinary study. These techniques include 2D and 3D microtomography (Micro-CT), confocal laser scanner microscopy (CLSM), atomic force microscopy (AFM), nanoindentation – Vickers hardness (Nano-VH) and X-ray fluorescence (XRF). They allow the measurement of claw structures on tiny scales, ranging from micrometres (μm) to nanometres (nm), providing identification and quantification of the chemical and structural elements that compose the bovine claw. Due to their specificity and sensitivity, they can help the scientific community, veterinary doctors and, therefore, rural producers to elucidate any enigmas concerning foot diseases not yet unveiled. Therefore, this new reality has emerged as a more rational line of research with the potential to explain the aetiopathogenesis of several foot diseases. In unravelling these enigmas, new opportunities to adopt more directed and effective preventive biosafety measures have emerged, as well as to minimise damage to breeders.

This study aims to review the literature concerning new technologies used to characterise the bovine claw microstructure and its importance in podiatry, highlighting the Micro-CT, CLSM, AFM, Nano-HV and XRF techniques.

Anatomy of the bovine claw

The claw is composed of keratinised epidermal tissue, which can be divided by its constitution, location and function. The wall, heel, sole, heel bulb, white line and the claw are parts of the whole structure (Figure 1). The feet are the extremities of the limbs, extending from the carpus or tarsus to the distal phalanges of fingers III and IV, separated in medial and lateral digits. The lateral digits present in the hindlimbs are larger than the medial digits, since they support a larger weight. In the forelimbs, the opposite occurs. The feet also have dewclaws or rudimentary digits, corresponding to fingers II and V (Schaller 1999; Bragula et al. 2004).

From a physiological point of view, it is believed that the horn tissue of some bovine and bubaline claws differ in their histochemical properties.

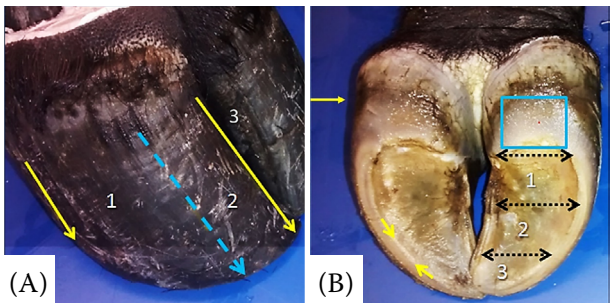

Figure 1. Claw anatomy

(A) Abaxial wall (1), dorsal wall (2), axial wall (3). (B) Heel (yellow arrow), sole (1, 2 and 3), heel bulb (blue square), white line (yellow arrows)

These properties, for example, involve the organisation of keratin and minerals present in the horny capsule of the claw (Assis et al. 2017a; Assis et al. 2017b). Thus, according to their consistency, they can be classified into hard and soft, varying according to the corresponding anatomical region. Usually, the horn of the bovine claw presents distinct regions of hardness and resistance, in the regions of the sole, heel and white line. The horny tissue that consists of the sole has a lower consistency, tending to have a softer aspect (Bragulla 2004; Greenough 2007). Nowadays, there are strong indications that the use of techniques that generate micro- and nanometric parameters, such as Micro-CT, CLSM, AFM, Nano-HV and XRF, can advance the study of the microstructure of the bovine claw (Assis et al. 2017a).

Regarding the sampling to perform the above-mentioned techniques, for analysis of biological material/tissue, a minimum of 30 samples is required for each analysis, as there is greater variation in the material. This takes the variation of each individual and the influence of the environment where they live into account. However, for metals or rocks, 3 to 6 samples are the minimum required, as there is less variation in the material (Fontelles et al. 2010).

Advanced techniques used in the microstructural characterisation of the bovine claw

2D AND 3D MICROTOMOGRAPHY (MICRO-CT)

Micro-CT has a similar principle to that of computed tomography. However, it allows the 360° rotation of the sample at the moment

https://doi.org/10.17221/167/2020-VETMED

of the evaluation and provides micro-scale values in a non-destructive process, with high-resolution power. The evaluation uses sequential slices of the sample through attenuation of X-rays, ranging from 360 to 490 sections (Lima et al. 2007). The analysis time extends according to the desired definition, ranging from 40 min to 8 h, to different biological materials (Coelho et al. 2012) and up to 32 h to analyse ceramics and metals. In the two-dimensional and three-dimensional microtomographic evaluation, it is possible to inspect the basic characteristics, such as the thickness, volume and porosity of the analysed tissue (Assis 2015; Rabelo et al. 2015). The microtomograph has a compact Micro-CT system for desktops, industrial, biomedical and quality control applications. The size of the X-ray tube focus is the distinction of this technique. This parameter can vary from 4 mm to 1 mm (normal focus), from 1 mm to 0.1 mm (minifocus) and from 100 µm to 1 µm (microfocus). The small diameter of the X-ray tube focus is a very important attribute of the Micro-CT (Lima et al. 2009).

The Micro-CT reveals details of the shape and chemical composition of the internal structures of materials, non-destructively, and with micrometric resolution. The longer the analysis time, the greater the precision and detail of the material studied on a micrometre scale. For the horny tissue of the claw, the average required time is 50 minutes. The horn case sample size can range from 1 mm to 70 mm (Assis et al. 2017a; Assis et al. 2017b).

It is possible to verify details up to 350 nanometres (nm) of the samples, whose size can reach 75 mm in diameter and 70 mm in length (Bruker 2013). Researchers have described the microtomography technique, using the SkyScan 1272® – Bruker microtomograph (Lopes et al. 2012; Bruker 2013; Assis et al. 2017b). This equipment sets the samples in a circular template, in order to obtain a vertical alignment, avoiding displacements during the angular movement and to maintain the visual field of a radiation detector – charge-coupled device (CCD) camera (Bruker 2013). The images acquired by the CCD camera are stored in a computer (1) for the standard configuration of the analysed object.

The analysis standardisation varies according to the analysed material. The equipment operator performs the material calibration according to the precision and specificity of what is being investigated. Therefore, calibration tests are carried out for each material, generating a standard that achieves the best quality of the images. After this standardisation, there is no manipulation of the results required, since each software performs the identification of both quantitative and qualitative structures from the same calibration in which the best images were generated. For the horny capsule, this calibration follows the orientation of what is already known from the structures already known through histological tests (Bruker 2013).

Following the above, the images are sent to a second computer (2) where the microstructural quantification occurs, along with the 2D reconstruction (pixel), 3D (voxel) and realistic visualisation by surface and volume rendering. Finally, with the use of a third computer (3), the images are treated through various software (CTvox, DATAviewer, CTan and CTvol). The Micro-CT can be equipped with an automatic sample exchanger (additional piece) and being connected to the front of the sample chamber. It can also be equipped with a graphics processing unit server (the process by which the final product of any digital processing is obtained) with eight NVIDIA Tesla graphic cards for accelerated 3D reconstruction of large slices (Lima et al. 2007; Lima et al. 2009). The 2D and 3D analyses of the microstructural parameters are executed in the software programs DataViewer, CTvox, CTan and CTvol (Assis 2015; Rabelo et al. 2015; Assis et al. 2017b) (Figure 2).

Given the importance of this technique, it covers many areas. Thus, studies demonstrate the use of Micro-CT in the field of odontology (Coelho et al. 2012), orthopaedics (Roche et al. 2012; Regnault et al. 2017), materials engineering (Zhu et al. 2011; Renghini et al. 2013; Miller et al. 2014), agronomy (Calistu et al. 2016) and biomaterials (Coelho et al. 2012; Santos et al. 2013). Recently, the technique has been used in veterinary medicine for the experimental evaluation of lungs (Lovric et al. 2013) and rat embryos (Tesarova et al. 2016), congenital malformations in reptile bones (de Carvalho et al. 2017) and embryonic structures of fish, molluscs and small insects (Metscher 2013). It is also important to note the application of Micro-CT in the study of bovine podiatry (Rabelo et al. 2015; Assis et al. 2017a; Assis et al. 2017b).

The results of Micro-CT in the study of bovine podiatry are innovative and possess great relevance in the attempt to unveil questions about the arrangement and organisation of keratin in bovine claws.

https://doi.org/10.17221/167/2020-VETMED

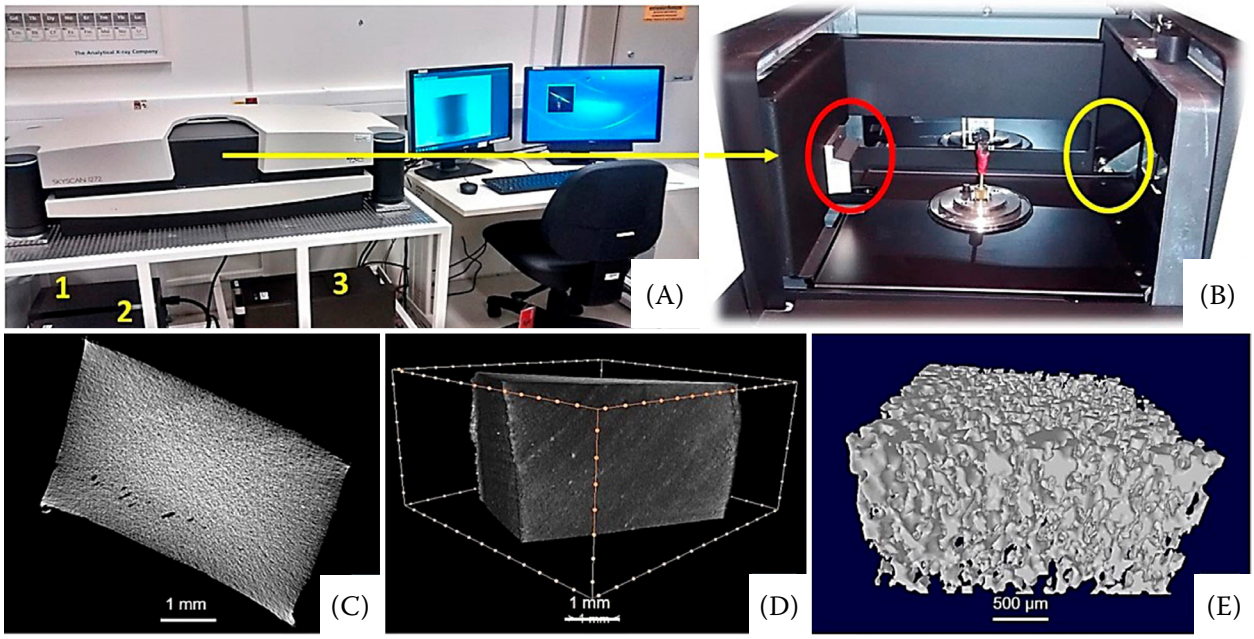

Figure 2. Micro-CT system – SkyScan 1272

(A) Micro-CT system with three computers to store and render images in 2D and 3D. (B) Yellow circle – X-ray micro system; red circle – CCD camera. (C) 2D image (DataViewer). (D) 3D reconstruction (CTvox). (E) Horn sample of bubaline hoof (CTan – CTvol)

Source: Images (A) and (B), adapted from Assis (2015); (C–E) Personal archive

Researchers have demonstrated through the 2D reconstruction of claws that the keratin is arranged in an intratubular and extratubular manner, and it is compact, with the absence of pores. In the studies, a colorimetric scale identified regions of higher and lower density of intra and extratubular keratin. It was observed that on a decreasing scale of density, the dorsal wall is denser, followed by the abaxial wall and, finally, the sole presents the lowest density (Figure 3). The findings suggest that these differences could be associated with a larger body mass being overweight on the walls, whereas, due to the sole being an impact absorption region, it presents with lower density (Assis 2015; Assis et al. 2017a; Assis et al. 2017b).

Through a 3D reconstruction, it was verified that the keratin is organised concentrically, forming helical horn tubules that present different angulations in the dorsal and abaxial walls and sole (Assis 2015; Assis et al. 2017a), as shown in Figure 4.

Studies about the equine claw, assessed by polarised light microscopy, showed that intratubular keratin is linear in nature (Kasapi and Gasoline 1997). The results also showed that the claw is subdivided into six regions (Ia – Ib, IIa – IIb and IIIa – IIIb) composed of distinct horn tubules, being the extratubular keratin organised in up to nine layers of helical lamellae at several angles. It should be noted that the presence of these lamellae has not been described in the bovine claw to the present time.

In cattle, Micro-CT quantified the number of horn tubules per mm^2, as well as the percentage of the different diameters of these tubules present in the dorsal wall, abaxial wall and sole of the claw (Assis 2015; Assis et al. 2017a). The diameters ranged from 17 µm to 153 µm. In bubalines, the digits of the forelimbs presented a higher percentage of larger diameter horn tubules.

On the other hand, the digits of the hindlimbs presented a higher percentage of smaller diameter tubules.

This is particularity related to the type of pressure exerted on each member and the type of joint that they possess, which can influence the synthesis and organisation of keratin and the resistance of the claw.

The study also revealed that the forelimbs support greater overweight body mass and have a ligamentous joint that absorbs larger impacts, whereas the hindlimbs present a bone joint, which increases the impact on the digits of the limb (Bragulla et al. 2004; Greenough 2007).

https://doi.org/10.17221/167/2020-VETMED

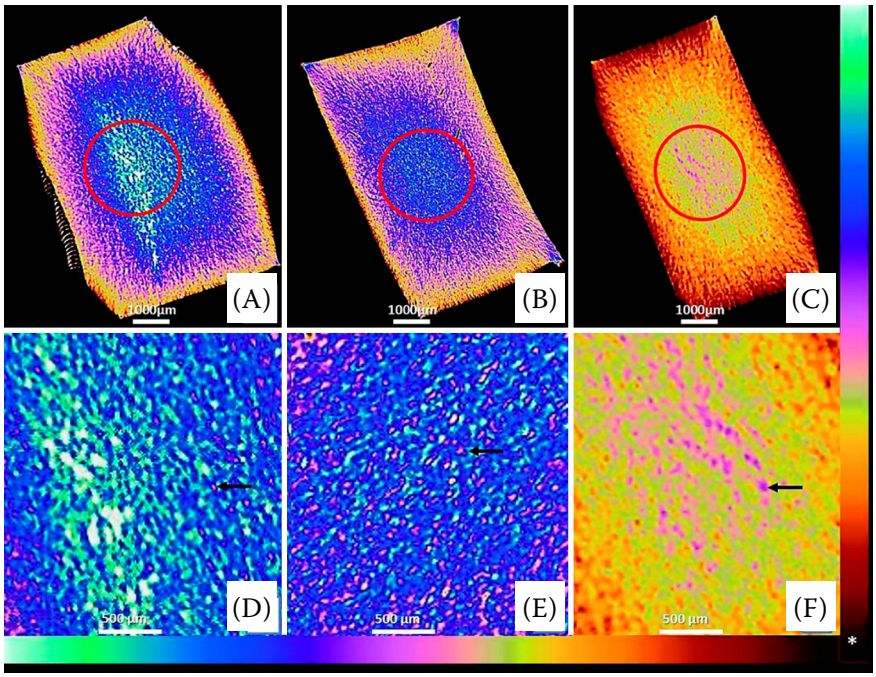

Figure 3. 2D microtomography of the bovine hoof
(A) Dorsal wall. (B) Abaxial wall. (C) Sole. (D and E) Dorsal and abaxial wall of the hoof, respectively, showing the intratubular keratin in pink and the extratubular keratin in blue and light green (black arrows), indicating a lower density of intratubular keratin in relation to the extratubular keratin. (F) Sole, the intratubular keratin is in blue-lilac (black arrow) and the extratubular keratin is in yellow, indicating the higher density of the intratubular keratin in relation to the extratubular keratin. The white asterisk (*) represents the colorimetric scale
Source: Adapted from Assis (2015)

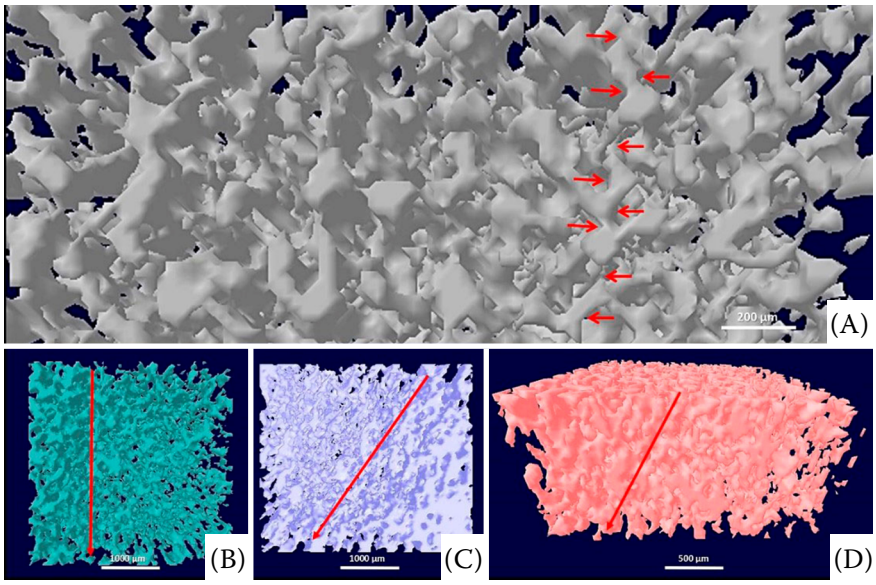

Figure 4. Microtomographic images of the bubaline digits hoof, indicating angulation of the horn tubules
(A) Red arrows – helical intratubular keratin of the horn tubules. (B) Red arrow – 90° angle. (C) Red arrow – 55° angle. Both angles in relation to the coronary corium. (D) Red arrow – 70° angle, in relation to the laminar corium
Source: Adapted from Assis et al. (2017b)

CONFOCAL LASER SCANNING MICROSCOPY – PROFILOMETRY (CLSM)

Confocal laser scanning microscopy was developed uniting an optical microscope with a laser beam, aiming to obtain high-resolution images through optical sections (Santhiago et al. 2016). CLSM is a piece of equipment that measures and evaluates thicker samples using a deep focus and allowing real-time 3D reconstruction "*in vivo*" (Andrade et al. 2015). This analysis makes it possible to evaluate bacterial biofilms, fungal structures, dental tissues, several cell types (Mendes et al. 2015) and fluorochrome marked tissues by immunofluorescence (Duajie 2017). CLSM (3D VK-X200®; Keyence) emits a laser beam that passes through the X-Y and Z optical scanning system through the surface of the sample. Then, the laser captured element obtains the height and depth data, based on the intensity of the reflected light, just for the sites in focus, by the confocal optical system. Therefore, the focal point of the Z axis is located according to the intensity of the reflected light, which allows one to capture a totally focused

https://doi.org/10.17221/167/2020-VETMED

image and define its height. Simultaneously, the obtained sections are stored and this stage is repeated when evaluating different sites (Duajie 2017).

After scanning the sample, the data is obtained through the software – VK Analyzer – to reconstruct the 2D images (laser and optic), then finally, for the 3D reconstruction. In addition to the images, the CLSM system reveals the surface roughness values of the analysed sample (Santhiago et al. 2017). The following are used in the system: Rp – the maximum height of the highest peak of the roughness, located above the midline; Rv – the maximum depth of the deepest valley of the roughness, located below the midline; Rz – the mean of the highest peaks, representing the height between the maximum and minimum points of the profile; and Ra – arithmetic roughness, which represents the mean of all points. However, it may not give a straight indication of the surface state. Therefore, Rq – roughness (Rms) is used, a parameter corresponding to Ra. Rq is the mean square deviation, which increases the effect of the irregularities that deviate from the mean and, thus, delineate the most reliable profile of the sample (Duajie 2017).

This technique has been used experimentally to evaluate the organisation and roughness of the outermost keratin layer of the bovine claw using a micrometric scale, in order to complement the data generated by the Micro-CT and AFM (nanometric), identifying possible fragility points (Assis et al. 2017b). In Figure 5, a 2D reconstruction of a healthy albino buffalo claw can be observed.

Figure 5. 2D analysis of albino bubalines by CLSM
The 2D reconstruction is observed (laser + optic). A horn tubule is seen in the white circle
Source: Adapted from LNNano – Laboratório Nacional de Nanotecnologia (2017) – Personal archive

ATOMIC FORCE MICROSCOPY (AFM)

Atomic force microscopy (AFM) is a nanotechnology that complements the microtomography and confocal laser scanning microscopy. Developed in 1986 by German researchers, it performs the microstructural characterisation of several structures with a nanometric resolution (Nanosurf FlexAFM 2017). This technique provides data on the topography and elasticity of the samples; however, it is restricted to electrically conductive surfaces. AFM is also employed in several areas, including characterisation of biological structures (Dufrene et al. 2013), viscoelastic properties in cancer cells (Rebelo et al. 2013) and it can also be extrapolated to studies in physics, chemistry (Alsteens et al. 2012) and materials engineering (Wagner et al. 2012; Wang et al. 2012). AFM is a probe scanning technique *raster scan* – linear, which can be composed of silicon, gold or diamond and measures forces smaller than 1 µN (micro-Newton) in the x, y and z directions (Rebelo et al. 2013). It should be noted that the scan occurs at a very small distance (1 nm) between the tip and the analysed sample, which makes it possible to scan on an atomic range (Dufrene et al. 2013).

To perform the AFM, a scanning probe microscope (SPM) is used, NX-10 (Park Systems, Suwon, Korea) – AFM mode – intermittent contact (tapping mode). The most commonly used tips are composed of silicon and are aluminium-coated on the back, the NCHR model (Nano World), with a normal force constant of 42 N/m and nominal resonance frequency of 320 kHz, being kept at a reflection beam – *cantilever* (Zamiri et al. 2017). To perform the analysis, the sample surface should be clean, flat, fixed on a metal disk by glue (*lift off*), and then inserted into the vacuum system. The tip of the probe is then positioned over the sample at a distance of 1 nm and the scan area is determined. A laser beam is emitted on the tip, which transmits a vibration amplitude on the sample, reflecting a repulsive force, increasing the resonance frequency on the tip. This force is reflected on the photodetector (light semiconductor) in a deflection system (natural position deviation). Thus, this amplitude of vibration initiates a feedback cycle that maintains the constant interaction of the sample and probe, changing the height of the tip (Figure 6). The output of this feedback cycle corresponds to the height of the local sample. At the end

https://doi.org/10.17221/167/2020-VETMED

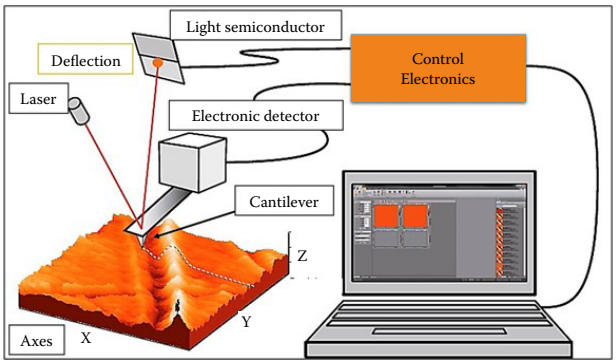

Figure 6. Laser scanning system – atomic force microscopy (AFM)

Incidence of the laser on the tip and its interaction with the sample, emitting the vibration force captured by the light semiconductor, causing positive feedback on the tip, which measures the topography of the area

Source: Adapted from Nanosurf FlexAFM (2017, p. 332)

of the scanning, with the acquired data, it is possible to reconstruct the 2D and 3D topography of the analysed surface and use the software to calculate the roughness (Wagner et al. 2012; Zamiri et al. 2017; Nanosurf FlexAFM 2017).

The AFM technique has been used experimentally in the microstructural characterisation of a healthy bubaline and bovine claw, supplemented with biotin or not (Cruz et al. 2017). This technique is able to delineate the microstructural parameters of normality in a nanometric scale, rugosity (Nanosurf FlexAFM 2017), and to expose the effects that biotin exerts on the keratinisation of the claw. Using this tool and the biotin supplementation, an increase in the sulfur content and a decrease in the calcium and potassium content in the abaxial claw wall were observed, also an increased percentage of the horn tubules showing smaller marrow diameters (17–51 µm) was visible, so the conclusion is that daily supplementation with 20 mg of biotin was able to promote alterations in the mineral composition and microstructure of abaxial claw wall in dairy cows, which may help to understand the function of biotin in the *stratum corneum* (Queiroz et al. 2021).

NANOINDENTATION – VICKERS HARDNESS (NANO-VH)

The Vickers nano-hardness test, in addition to the use in the study of the horn and claw of domestic animals (Abdullahi et al. 2014), can also be applied to metals used in materials, aeronautics and civil engineering (Ghassemi-Armaki et al. 2014). The use of this technique in bovine podiatry has been used recently and has allowed the acquisition of data about the Vickers hardness and the elastic modulus of the different regions of the claws of horses (Sargentini et al. 2012; He and Huang 2015), bubalines (Assis et al. 2017b) and cattle (Assis et al. 2017a). The samples are prepared for Nano-VH with the tissue being wrapped in a polymer resin, resin T208 (Cristal®), a styrene monomer, the catalyst MEK TGDM50 and dimethylamine, proportionally for hardening in approximately three minutes, to check the stability of the sample. After the resin is dried, surface abrasion is promoted, using sandpaper with a grit ranging from 80 to 2 500 (Politriz Arotec; Aropol E®), in order to expose the surface of the sample. Sequentially, the Nano-indentor measures the Vickers hardness and the elastic modulus (Mechanical Tester PB1000®; Nanovea, Irvine, CA, USA) (Fischer-Cripps 2011).

The sample is subjected to a force load (milliNewton – mN – unit of force) in a period of time (in seconds). Then, the force, at its maximum load, is removed (variable for each material). The Vickers hardness is calculated from the indentation load divided by the projected contact area and the elastic modulus is determined from the slope of the maximum load and discharge curve (Lopes et al. 2012; Ghassemi-Armaki et al. 2014), as shown in Figure 7.

A greater elastic modulus was observed in the vertical direction of the horn tubules in a cross section, demonstrating that the claw behaves

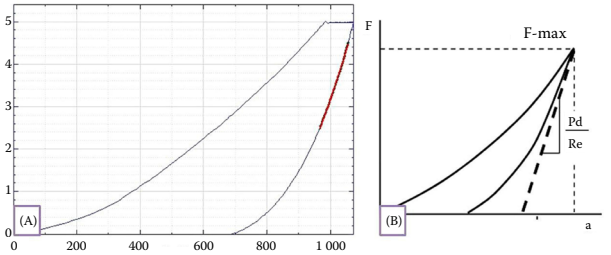

Figure 7. Representative graphs of the nano-hardness test

(A) The maximum load and discharge curve. (B) F-max – maximum force load applied to the sample

a = the projected contact area; Pd/Re ratio = penetration power/elastic recovery, which determines the elastic modulus

Source: Adapted from Assis (2015) and Fischer-Cripps (2011, p. 282)

https://doi.org/10.17221/167/2020-VETMED

as a spring in order to absorb the impact when the animal touches the ground. It is important to say that similar information had only been described in the equine claw (Kung 1991). Also related to the equine claw, the study revealed a lower tensile strength in the tubule cross section when compared to the horizontal axis.

X-RAY FLUORESCENCE (XRF)

The X-ray fluorescence technique (XRF) adds the results of the other techniques described above. It detects chemical elements from sodium (Na) to uranium (U), non-destructively, with a penetration power of 3 mm to 5 mm. Thus, XRF provides a fluorescence spectrum with peaks of the energy released by each element, which are then identified by software and then quantified, according to the chosen parameters. This analysis allows the surface evaluation of soil, metal and biological material samples, such as the bovine claw (Assis 2015). An analysis to quantify the minerals present in a bubaline claw was performed (Assis et al. 2017b; Queiroz 2021), such as sulfur (S), calcium (Ca), potassium (K), phosphorus (P), zinc (Zn) and copper (Cu).

For these analyses, a Shimadzu EDX – 720X-ray fluorescence spectrometer was used with a rhodium (Rh) tube, 10 mm collimates, 15 kV voltage, 100.0 uA current and 30 pass pressure. The samples are placed in the machine through a sample holder with a rotating base and are excited by X-rays, in order to stimulate the last layer of the electrons of the atoms of the chemical elements. Then, the electrons emit a fluorescent wavelength, which is captured by a diffractometer that identifies the corresponding element and quantifies its percentage in the analysed sample. Data files provided by the diffractometer are saved in text files (txt) and transformed into data files (dat), allowing the results to be presented in the form of angle graphs (2θ) vs. (u. a. – Intensity), using the EDX-GP software (Bajanowski et al. 2001; Assis 2015) (Figure 8).

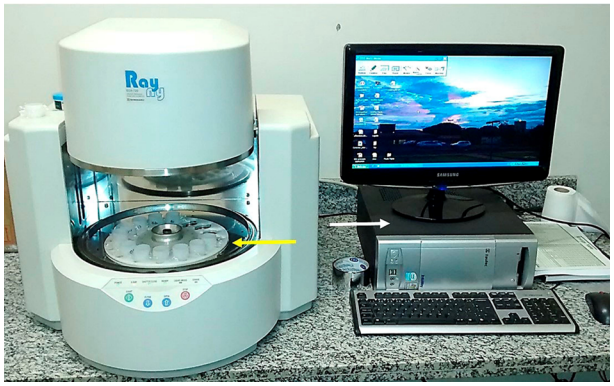

Figure 8. Equipment for the non-destructive biochemical analysis by energy dispersion EDX-720 (EDXS – X-ray fluorescence)

The sample holder with a rotating base is indicated by the yellow arrow. The white arrow points at the computer used for the data conversion through the EDX-GP software

Source: Personal archive

Using the XRF technique, researchers quantified the average percentage of the minerals present in the claw of the fore and hindlimbs of a bubaline (Assis et al. 2017a). The results indicated the presence of 83.53% sulfur (S), 8.13% calcium (Ca), 3.47% potassium (K), 3.74% phosphorus (P), 0.81% zinc (Zn) and 0.31% copper (Cu) in the samples. They also observed that the lateral digits of the hindlimbs present a higher concentration of phosphorus when compared to the medial digits of the same limb. However, the medial and lateral digits of the hindlimbs showed no difference. Another feature worth mentioning is that the lateral digits of the hindlimbs deposit more sulfur than the lateral digits of the forelimbs, which, in turn, deposit more calcium. It should be emphasised that the medial digits of the fore and hindlimbs do not portray any difference. These characteristics are correlated with the body mass overload deposited on the different digits. Thus, the structures that receive a higher overload tend to deposit more S and the other regions deposit more Ca. The regions that deposit higher concentrations of S are more resistant (Assis et al. 2017a). Study made by Assis et al. (2017c) also emphasised the practicality of this technique, since there is no need to grind the samples, which is considered difficult since the claw capsule presents a solid and hardened consistency.

The methods described in Table 1 work on different scales, complementing information and showing the same claw structures in different areas, from the micrometric scale to the atomic range. In decreasing order, Micro-CT is mentioned in a micrometre scale, AFM, CLSM and Nano-VH in a nanometre scale and finally XRF in an atomic scale. In this sense, they make it possible to accurately assess the tissue and cellular microstructure of the bovine claw. Furthermore, it makes it possible to address anatomical, nutritional, biosecurity and animal

https://doi.org/10.17221/167/2020-VETMED

Table 1. Claw parameters verified by means of microtomography (Micro-CT), atomic force microscopy (AFM), confocal laser scanner microscopy (CSLM), nano-indentation (Nano-VH) and X-ray fluorescence (XRF) techniques

Samples/ techniques	Micro-CT	AFM	CSLM	Nano-VH	XRF
Sample size	1 cm^2	1 cm^2	1 cm^2	1 cm^2	1 cm^2
Resolution scale	µm	nn/atom	nn	nn	atom
Morphometrics	horn tubules: from 17–150 µm for pigmented buffaloes and cattle; 17–119 µm for albino buffaloes	surface roughness of keratinocytes of the claw capsule	claw capsule tissue surface roughness	Vickers hardness of the claw capsule in the longitudinal and cross sections	percentage of mineral elements present in the claw capsule
Obtained volume	0.001–0.051 mm^3	–	–	–	–
Estimated time of analysis	50'–32 h	15'–30'	5'	1'	2.5'
Evaluated tissues	claw capsule	claw capsule	claw capsule	claw capsule	claw capsule
Pros	easy sample preparation and analysis, excellent resolution and reconstruction of 2D and 3D images; provides quantitative data for various sample measurement parameters	analyses surfaces on the nanometre scale	ease of performing the analysis, even with samples with very irregular surfaces	evaluates Vickers hardness and elastic modulus of the claw with ease	technique that allows one to evaluate the mineral elements present in the claw capsule without destroying the sample; in addition to the reduced time in the execution of the analysis
Cons	the time taken to analyse the samples is usually four times the time to analyse each sample	difficulty analysing a surface as rough as the claw; this increases the analysis time by up to three times per sample	little equipment available for the analysis	time of 3 h to 4 h for the preparation of each sample	the sample needs to be very well prepared and without contamination, as this technique even detects dirt on the surface of the sample

welfare issues within bovine production systems in a multidisciplinary way. The results of these techniques, which evaluated the cattle and bubaline claw, are presented in Table 2.

Regarding the relationship between the histology and the Micro-CT, it should be noted that the Micro-CT can be used both for analysis of the claw and bones of animals. In the case of animals with bone density problems due to decalcification, this technique is ideal for assessing the volume of the lost bone. Moreover, the result of the analysis of the law capsule is directly related to the integrity of the tissue of the coronary corium composed of the dermis and dermal papillae and analysed by the histology technique. Dermal papillae are known to synthesise keratin that gives direction to the claw growth. In this sense, if there is a histological change in these structures, there will be a change in the quality of the claw capsule, as evidenced by the Micro-CT results.

However, other areas of veterinary medicine still need high-tech tests and can use these techniques to generate qualitative and quantitative patterns of the tissues. For example, soft tissues and cells, sebaceous glands in the foreskin of bulls, evaluation of the bones and teeth of dogs with dental problems.

Moreover, it should also be noted that there is a need to test these analyses in other species that also present with foot injuries, such as sheep, goats and swine.

https://doi.org/10.17221/167/2020-VETMED

Table 2. Vickers hardness and mean elastic modulus of the hoof of the Jafarabadi Bubaline and Girolando cattle, in cross and horizontal sections of the dorsal wall, abaxial wall and sole

Nanoidentation	Vickers hardness	Elastic modulus
Girolando cattle		
Cross section	29.566 ± 2.696	5.461 ± 0.089
Horizontal	29.233 ± 4.316	4.552 ± 0.522
Mean	29.33	4.65
J. Bubaline		
Cross section	26.07 ± 4.66	5.12 ± 0.12
Horizontal	26.42 ± 3.19	4.57 ± 0.20
Mean	25.74	4.65

Source: Values adapted from Assis et al. (2017a) and Assis et al. (2017b)

AFM	T0 (Rms)	T1 (Rms)
Jersey and Holstein-Friesian crossing cattle		
Abaxial wall	124.55 ± 56.24 nm	92.69 ± 50.00 nm

Source: Adapted from Cruz et al. (2017)

Micro-CT	17 µm	51 µm	85 µm	119 µm	153 µm
J. Bubaline					
FL-medial	37.23 ± 9.46[a]	49.16 ± 2.16[a]	10.85 ± 7.17[a]	2.56 ± 0.97[a]	0.03 ± 0.01[a]
HL-lateral	43.25 ± 2.48[a]	50.34 ± 0.66[a]	6.06 ± 0.43[a]	0.35 ± 0.34[b]	0.00 ± 0.00[a]

Source: Adapted from Assis et al. (2017b)

XRF	S (%)	Ca (%)	P (%)	Zn (%)	Cu (%)
J. Bubaline					
FL	82.8 ± 3.5[a]	8.70 ± 2.41[a]	3.85 ± 0.56[a]	0.79 ± 0.13[a]	0.31 ± 0.04[a]
HL	84.2 ± 2.3[a]	7.57 ± 1.08[a]	3.64 ± 0.39[a]	0.82 ± 0.07[a]	0.31 ± 0.03[a]

Source: Adapted from Assis et al. (2017b)

Mean and standard deviation of the quadratic roughness by atomic force microscopy from the hooves of Jersey and Holstein-Friesian crossing heifers, before and after biotin supplementation; [a]Mean and standard deviation of the percentage horn tubules present in the hooves of the Jafarabadi buffaloes; [b]Mean and standard deviation of the percentage of minerals present in the Jafarabadi buffalo hoof

AFM = atomic force microscopy; FL = forelimb; HL = hindlimb; J. Bubaline = Jafarabadi Bubaline; Micro-CT = microtomography; Rms = roughness; XRF = X-ray fluorescence

Conclusion

The technologies Micro-CT, CLSM, AFM, Nano-VH and XRF allow for the elucidation of factors related to the morphological and pathological microstructure of the claw, both in animals resistant and susceptible to foot diseases. Microstructural analyses of the claw can be performed on a micro and nanometric scale, having a high-resolution image, generating atomic range data non-destructively.

The use of these modern techniques as an alternative in the study of large ruminants podiatry will have undisputed importance and can be used as tools to increase the morphofunctional data about the locomotion system of production animals. It can also be used in the analysis of the efficiency of different therapeutic protocols that are used to prevent and treat foot diseases.

It is believed that the difficulties in using some of the described techniques are limited to the availability of the equipment associated with a high number of samples. However, the results of each of them reveal information of the indisputable importance for bovine podiatry.

This new line of research represents new perspectives of potential discoveries and may generate

https://doi.org/10.17221/167/2020-VETMED

important tools for the better understanding and explanation of bovine podiatry, constituting a more rational and comprehensive line of research to explain mechanisms related to the aetiopathogenesis of podal diseases and assist in the adoption of more targeted and effective preventive biosafety measures.

Conflict of interest

The authors declare no conflict of interest.

REFERENCES

Abdullahi U, Salihi A, Ali AB. Hardness behaviour of thermoplastic cattle horn using nanoindentation technique. Asian J Engineer Technol. 2014 Apr;2(2):169-73.

Alsteens D, Dupres V, Yunus S, Latge JP, Heinisch JJ, Dufrene YF. High-resolution imaging of chemical and biological sites on living cells using peak force tapping atomic force microscopy. Langmuir. 2012 Dec 11;28(49):16738-44.

Andrade JP, Mercurio DG, Campos PMBGM. Avaliacao celular das estruturas cutaneas por meio da microscopia confocal de reflectancia [Evaluation of cutaneous cellular structures by reflectance confocal microscopy]. RBM Rev Bras Med. 2015;71:5-14. Portugues.

Assis BM. Histomorfometria, microtomografia bidimensional e tridimensional, teste de nanodureza e composicao bioquimica do estojo corneo de bubalinos [Histomorphometry, bidimensional and tridimensional microtomography, nanohardness test and biochemical composition of hoof capsule of buffaloes] [PhD thesis]. Goiânia, Goiás: Universidade Federal de Goiás; 2015. 81 p. Portuguese.

Assis BM, Silva LAF, Lima CRO, Sant'Ana FJF, Santos GP, Vulcani VAS, Rabelo RE. Microtomographic parameters and nanoindentation of the hoof of Girolando cattle. Anat Histol Embryol. 2017a Oct;46(5):456-63.

Assis BM, Silva LAF, Lima CRO, Gouveia RF, Vulcani VAS, de Sant'Ana FJF, Rabelo RE. Microstructure and hardness of buffalo's hoofs. Anat Histol Embryol. 2017b Oct;46(5): 439-45.

Assis BM, Vulcani VAS, Silva LAF, Dias M, Pancotti A, Lima CRO, Rabelo RE. Biochemical composition of the hoof capsule of buffaloes and its influence on hoof quality. Arq Bras Med Vet Zootec. 2017c Feb;69(1):57-64.

Bajanowski T, Kohler H, Schmidt PF, von Saldern CF, Brinkmann B. The cloven hoof in legal medicine. Int J Legal Med. 2001;114(6):346-8.

Bragulla HKD, Budras G, Mulling S, HE Konig. Forelimb or thoracic limb (membra thoracica). In: Konig HE, Bragulla HKD, editors. Veterinary anatomy of domestic animals. Stuttgart: Schattauer Verlag GmbH; 2004. p. 1-48.

Bruker. Bruker microCT – User manual. Desk-top X-ray microtomograph SkyScan 1272 [Internet]. 2013 [cited 2020 Mar 2]. Available from: https://www.comef.com.pl/upload/pdf/bruker/SkyScan%201272.pdf.

Calistu AE, Cara IG, Topa D, Jitareanu G. Analyzing soil porosity under different tillage systems using X-ray microtomography. Lucr Stiint (Ser Agron). 2016;59(1):201-4.

de Carvalho MPN, Sant'Anna SS, Grego KF, de Campos Fonseca-Pinto ACB, Lorigados CAB, Queiroz-Hazarbassanov NGT, Catao-Dias JL. Microcomputed tomographic, morphometric, and histopathologic assessment of congenital bone malformations in two neotropical viperids. J Wildl Dis. 2017 Oct;53(4):804-15.

Coelho PG, Giro G, Kim W, Granato R, Marin C, Bonfante EA, Bonfante S, Lilin T, Suzuki M. Evaluation of collagen-based membranes for guided bone regeneration, by three-dimensional computerized microtomography. Oral Surg Oral Med Oral Pathol Oral Radiol. 2012 Oct;114(4):437-43.

Cruz AF, Queiroz PJB, Assis BM, Silva DC, Rabelo RE, Silva LAF. [Use of atomic force microscopy (AFM) to evaluate the surface microstructure of the abaxial wall of the hoof of calves supplemented with biotin – Partial results]. In: II Encontro Cientifico da Escola de Veterinaria e Zootecnia da Universidade Federal de Goias, 2017, Goiânia-GO. Anais do II Encontro Científico da Escola de Veterinária e Zootecnia da Universidade Federal de Goiás. Goiânia-GO: Escola de Veterinária e Zootecnia da Universidade Federal de Goiás; 2017; p. 174-9. Portuguese.

Duajie L. Manual, a better mensure. Textile texture measurement using 3D profilometry [Internet]. 2017 [cited 2020 Mar 2]. Available from: https://nanovea.com/AppNotes/textile-texture.pdf.

Dufrene YF, Martinez-Martin D, Medalsy I, Alsteens D, Muller DJ. Multiparametric imaging of biological systems by force-distance curve-based AFM. Nat Methods. 2013 Sep;10(9):847-54.

Fischer-Cripps AC. Nanoindentation – Hardcover. New York: Springer International Publishing; 2011. 282 p.

Fontelles MJ, Simoes MG, Almeida JC, Fontelles RGC. Metodologia da pesquisa: Diretrizes para o calculo do tamanho da amostra [Scientific research methodology: Guidelines for size sample calculation]. Rev Para Med. 2010;24(2):57-64. Portuguese.

Freitas SLR. Venografia dos digitos de animais jovens antes e apos aplicacao intrarruminal de oligofrutose [Venographic study of foot of young bovine before and after intrarruminal oligofructose application] [Master thesis].

https://doi.org/10.17221/167/2020-VETMED

Goiânia, Goiás: Universidade Federal de Goiás, Escola de Veterinária e Zootecnia; 2015. Portuguese.

Ghassemi-Armaki H, Maaß R, Bhat SP, Sriram S, Greer JR, Kumar KS. Deformation response of ferrite and martensite in a dual-phase steel. Acta Mater. 2014;62:197-211.

Greenough PR. Bovine laminitis and lameness – A hands on approach. Philadelphia: Sounders Elsevier; 2007. 311 p.

He BB, Huang MX. Revealing the intrinsic nanohardness of lath martensite in low carbon steel. Metall Mater Trans A Phys Metall Mater Sci. 2015;46(2):688-94.

Kasapi MA, Gosline JM. Design complexity and fracture control in the equine hoof wall. J Exp Biol. 1997 Jun;200 (Pt 11):1639-59.

Kung M. Die Zugfestigkeit des Hufhorns von Pferden. Messungen an definierten Stellen des Hufes sowie unter dem Einfluss verschiedener Umgebungsbedingungen [Tensile strength of the hoof horn of horses. Measurements at defined points on the hoof and under the influence of various environmental conditions] [PhD thesis]. Switzerland: University of Zürich; 1991. German.

LNNano – Laboratório Nacional de Nanotecnologia. Microscopia a laser confocal (perfiolometria) [Internet]. 2017 [cited 2020 May 2]. Available from: https://lnnano.cnpem.br/sobre-o-lnnano/.

Lima I, Appoloni C, Oliveira LC, Lopes RT. Caracterizacao de materiais ceramicos atraves da microtomografia computadorizada 3D [Characterization of ceramic materials through 3D computerized microtomography]. Rev Bras Arqueometria, Restaur Conserv. 2007;1(2):22-7. Portuguese.

Lima I, Lopes RT, Oliveira LF, Alves JM. Analise de estrutura ossea atraves de microtomografia computadorizada 3D [Bone structure analysis using 3D computed microtomography]. Rev Bras Fís Méd. 2009;2(1):6-10. Portuguese.

Lopes AP, Fiori AP, Reis Neto JM, Marchese C, Vasconcellos EMG, Trzascos B, Onishi CT, Pinto-Coelho CV, Secchi R, Silva GF. Analise tridimensional de rochas por meio de microtomografia computadorizada de raios-x integrada a petrografia [X-ray microtomography as tool for microstructural and mineral phase analysis]. Geociencias. 2012;31(1):129-42. Portuguese.

Loureiro MG. Estudo da tecnica de venografia dos digitos de vacas [Study of venography technique in digits of cows] [PhD thesis]. Botucatu: Universidade Estadual Paulista, Faculdade de Medicina Veterinária e Zootecnia; 2013. Portugues.

Lovric G, Barre SF, Schittny JC, Roth-Kleiner M, Stampanoni M, Mokso R. Dose optimization approach to fast X-ray microtomography of the lung alveoli. J Appl Crystallogr. 2013 Aug 1;46(Pt 4):856-60.

Mendes FBR, Castro RPR, Macedo MP, Pinto CAL, Duprat Neto JP, Rezze GG. Diagnostico de pseudomelanoma na microscopia confocal: O desafio das celulas dendriticas epidermicas [Pseudomelanoma diagnostic through confocal microscopy: The challenge of the epidermal dendritic cells]. Surg Cosmet Dermatol. 2015;7(3):246-8. Portuguese.

Metscher BD. Biological applications of X-ray microtomography: Imaging micro-anatomy, molecular expression and organismal diversity. Microsc Anal (Am Ed). 2013 Mar;27 (2):13-6.

Miller KJ, Zhua W, Laurent GJ, Glenn M, Gaetanib A. Experimental quantification of permeability of partially molten mantle rock. Earth Planet Sci Lett. 2014;388(2): 273-82.

Nanosurf FlexAFM. Manual operating instructions for C3000 control software version 3.6. Switzerland; 2017. 332 p.

Queiroz PJB, Assis BM, Silva DC, Noronha Filho ADF, Pancotti A, Rabelo RE, Borges NC, Vulcani VAS, Silva LAFD. Mineral composition and microstructure of the abaxial hoof wall in dairy heifers after biotin supplementation. Anat Histol Embryol. 2021 Jan;50(1):93-101.

Rabelo RE, Vulcani VAS, Sant'Ana FJF, Silva LAF, Assis BM, Araujo GHM. Microstructure of Holstein and Gir breed adult bovine hooves: Histomorphometry, three-dimensional microtomography and microhardness test evaluation. Arq Bras Med Vet Zootec. 2015 Nov-Dec;67(6): 1492-500.

Rebelo LM, de Sousa JS, Mendes Filho J, Radmacher M. Comparison of the viscoelastic properties of cells from different kidney cancer phenotypes measured with atomic force microscopy. Nanotechnology. 2013 Feb 8;24(5): 1-12.

Regnault S, Hutchinson JR, Jones ME. Sesamoid bones in tuatara (Sphenodon punctatus) investigated with X-ray microtomography, and implications for sesamoid evolution in Lepidosauria. J Morphol. 2017 Jan;278(1):62-72.

Renghini C, Giuliani A, Mazzoni S, Brun F, Larsson E, Baino F, Vitale-Brovarone C. Microstructural characterization and in vitro bioactivity of porous glass-ceramic scaffolds for bone regeneration by synchrotron radiation X-ray microtomography. J Eur Ceram Soc. 2013;33(9):1553-65.

Roche B, David V, Vanden-Bossche A, Peyrin F, Malaval L, Vico L, Lafage-Proust MH. Structure and quantification of microvascularisation within mouse long bones: What and how should we measure? Bone. 2012 Jan;50(1):390-9.

Santhiago M, Bettini J, Araujo SR, Bufon CC. Three-dimensional organic conductive networks embedded in paper for flexible and foldable devices. ACS Appl Mater Interfaces. 2016 May 4;8(17):10661-4.

Santhiago M, Strauss M, Pereira MP, Chagas AS, Bufon CC. Direct drawing method of graphite onto paper for high-

https://doi.org/10.17221/167/2020-VETMED

performance flexible electrochemical sensors. ACS Appl Mater Interfaces. 2017 Apr 5;9(13):11959-66.

Santos AC, Mendes CMC, Rosa FP. A microtomografia computadorizada aplicada a bioengenharia tecidual ossea com o uso de biomateriais [The X-ray microcomputed tomography applied to bioengineering bone tissue with the use of biomaterials]. Rev Cienc Med Biol, Salvador. 2013;12(4):478-81. Portuguese.

Sargentini C, Tocci R, Andrenelli L, Giorgetti A. Preliminary studies on hoof characteristics in Amiata donkey. Ital J Anim Sci. 2012;11(1):123-7.

Schaller O. Nomenclatura anatomica veterinaria ilustrada [Illustrated veterinary anatomical nomenclature]. São Paulo: Editora Manole Ltda; 1999. 614 p.

Silva LH. Morfometria radiografica e tomografica em digitos de bovinos e bubalinos [Radiographic and tomographic morphometry in digiti of the cattle and buffaloes] [Master thesis]. Goiânia, Goiás: Universidade Federal de Goiás, Escola de Veterinária e Zootecnia; 2012. Portuguese.

Tesarova M, Zikmund T, Kaucka M, Adameyko I, Jaros J, Palousek D, Skaroupka D, Kaiser J. Use of micro computed-tomography and 3D printing for reverse engineering of mouse embryo nasal capsule. J Instrum. 2016 Mar; 11(3):1-11.

Wagner C, Fournier N, Tautz FS, Temirov R. Measurement of the binding energies of the organic-metal perylene-teracarboxylic-dianhydride/Au111 bonds by molecular manipulation using an atomic force microscope. Phys Rev Lett. 2012 Aug 17;109(7):076102.

Wang QH, Kalantar-Zadeh K, Kis A, Coleman JN, Strano MS. Electronics and optoelectronics of two-dimensional transition metal dichalcogenides. Nat Nanotechnol. 2012 Nov;7(11):699-712.

Zamiri M, Anwar F, Klein BA, Rasoulof A, Dawson NM, Schuler-Sandy T, Deneke CF, Ferreira SO, Cavallo F, Krishna S. Antimonide-based membranes synthesis integration and strain engineering. Proc Natl Acad Sci U S A. 2017 Jan 3;114(1):1-8.

Zhu W, Gaetani GA, Fusseis F, Montesi LG, De Carlo F. Microtomography of partially molten rocks: Three-dimensional melt distribution in mantle peridotite. Science. 2011 Apr 1;332(6025):88-91.

Received: August 24, 2020
Accepted: March 7, 2022
Published online: May 27, 2022